Applied Energy 180 (2016) 472–482

Contents lists available at ScienceDirect

Applied Energy

journal homepage: www.elsevier.com/locate/apenergy

A simulation framework for prediction of thermoelectric generator system performance

Olle Högblom, Ronnie Andersson *

Department of Chemistry and Chemical Engineering, Competence Center for Catalysis, Chalmers University of Technology, SE-41296 Gothenburg, Sweden

HIGHLIGHTS

- Novel multiscale simulation framework for TEG systems at steady state conditions.
- Experimental validation including operation at highly non-ideal conditions.
- Allowing efficient modeling of thermoelectric effects.
- Two-way coupling of energy maintained in CFD analysis.

ARTICLE INFO

Article history:
Received 11 March 2016
Received in revised form 2 July 2016
Accepted 2 August 2016

Keywords:
Thermoelectric generator
Simulation
TEG
CFD
System
Subgrid model

ABSTRACT

This paper presents a novel framework for characterization and simulation of thermoelectric generator systems that allows accurate and efficient prediction of electric and thermal performance at steady state conditions. The simulation framework relies on regression analysis of single thermoelectric modules including voltage, current, temperatures and heat flow. A physical description of the main phenomena is included in models and enables accurate prediction of module performance over large ranges in temperature and current. Moreover it allows a system of modules electrically connected to be analyzed and used together with fluid dynamics simulations. When used in conjunction with CFD analysis it allows efficient modeling of electrical and thermal performance by simultaneous solution of the coupled equations for energy transport and thermoelectric power generation. This efficiency comes from the fact the modeling does not require full resolution as first principle simulations does. Therefore it solves the scale separation problem and allows multiphysics simulation with just a minor increase in computational power.

Experimental validation on a system consisting of electrically connected modules shows excellent prediction of heat flow as well as current and voltage. Validation confirms the simulation framework allows extrapolation outside the measured operating range used when developing the models. Even under highly non-ideal conditions with reversed current, i.e. when modules operate as Peltier coolers rather than generators, very reliable predictions are obtained.

Results show the simulation framework captures the main physics and allows efficient and reliable predictions. The models allow physical separation of heat conduction, Peltier, Joule and Seebeck effects and the different phenomena are studied and discussed in detail for various thermal loads and electrical configurations.

1. Introduction

Thermoelectric generators (TEG), which allows direct conversion of heat into electricity, are raising in popularity for heat recuperation applications mainly because of their compactness and robustness without moving parts. Different fields of implementation of TEGs have been studied, including biomass [1–3], solar energy [4–8], geothermal [9,10], nuclear [11], automotive [12–16] and even industrial power plants [17,18]. Due to the broad interest in developing technical applications effort is also made into developing simulation tools ranging from first principles simulations of small systems [19–23], to full scale TEG system simulations using simplified models [15,16] and also coupled system simulations by combining fluid dynamics simulations with thermoelectric models [24].

Although the equations describing the thermoelectric (TE) conversion inside the semiconducting materials are well known [25],

* Corresponding author.
E-mail address: ronnie.andersson@chalmers.se (R. Andersson).

http://dx.doi.org/10.1016/j.apenergy.2016.08.019
0306-2619/

Nomenclature

α	Seebeck coefficient, V/K
I	current, A
Π	Peltier coefficient, V
Ψ	combined Peltier and Thomson coefficients, V
R	resistance, Ω
T	temperature, K
τ	Thomson coefficient, V/K
U	voltage, V
Q	source term, W/m^3
Q	heat flow, W

Subscripts

avg	average between hot and cold side
c	cold side
h	hot side
int	internal
L	load
Si	seebeck where i = 1, 2
Ri	internal resistance where i = 1, 2, 3
Fi	fourier conduction where i = 1, 2
PTi	Peltier & Thomson where i = 1, 2

material data might be difficult to find. The performance of commercial modules can also vary depending on crystal orientation, small geometrical differences, and other properties that might be hard to determine in a commercial module [26]. For example the thermal and electrical contact resistances might vary significantly depending on process parameters and are usually not know [22]. The influence of electrical and thermal contact resistance can have an significant affect on module performance as shown in an investigation by Bjørk [27]. Ebling et al. [28] compare contact resistances resulting from use of different solders. They also present a technique for measuring electrical contact resistances within a TE module. The authors has recently proposed a method to determine both the electrical and thermal contact resistances in thermoelectric modules (TEM) using measurements and first principle simulations [29].

Although material data and internal contact resistances can be determined, thereby allowing a first principle simulation approach, this might be computationally too demanding even for computer clusters. A TEG system for a heavy duty automotive application could consist of up to hundred thousand internal parts, i.e. electrical connectors and semiconducting legs of *n*- and *p*-type. If the modules are subjected to different temperatures, no simplifications can be done and all internal parts would need to be resolved with good resolution to allow temperature dependent material data to be accounted for correctly in the simulations.

In most technical applications the heat source for the thermoelectric devices is provided by fluids, for automotive applications the waste heat in the exhaust gas, which means simulations tools for TEG systems need to account for both fluid dynamics and thermoelectric generation. Thereby requiring resolution of the flow field, e.g. turbulent flow and local heat fluxes in the fluid domain, in addition to resolution of the individual modules. Computational fluid dynamic (CFD) simulations can be used for optimizing design of TEG heat exchangers and predicting system performance [30,31]. The main advantage using CFD for analysis of TEG systems is that spatial and temporal variations of heat fluxes and temperature distributions can be resolved [19]. However, simulation of large TEG systems without introducing severe simplification in thermoelectric performance require fast and accurate subgrid TEG models to be developed for CFD analysis.

Several simplified models of TE generators has been presented in the literature and Fraisse et al. has summarized some of the most common approaches and compared these to first principle simulations [32]. The simplified models presented here are developed for TE legs and they require temperature dependent material data. They could in theory after some additional development be used to build subgrid models for CFD analysis but it would require additional closures such as thermal and electrical contact resistances. These models would in a CFD analysis of a large system of modules however be quite computational demanding since they require models for the individual TE legs.

Recently Montecucco and Knox developed a transient model for analysis of TE power generation accounting for electrical as well as thermal dynamics [33]. Implementation of this model on system of modules connected together, allows various connections in serial and parallel to be studied but requires identical temperature loads on the different modules. They also developed efficient models that can be used to simulate the electrical performance for large system of modules working at different but known thermal loads when connected in series and in parallel [34]. Following the strategy developed by Montecucco et al. a new model is proposed that allows a wider range of operating conditions to be simulated by introducing more physical models. More importantly the aim of the present work is to introduce a novel model allowing heat flow coupled with the electric current in a large system of modules to be predicted in an efficient way. This would provide a generic simulation framework that allows both large systems, possibly containing modules of different types, to be accounted for in an efficient and physical correct way while maintaining two-way coupling of the energy flow between the TEG system model and a CFD model. The framework presented in this paper is therefore developed as a remedy to the lack of TEG system models that can be implemented in CFD analysis. A comparison between the different modeling strategies discussed above is summarized in Fig. 1.

By modifying Montecucco electrical models to include more physics and by adding additional models describing the thermal fluxes, the goal is thus to contribute with a novel simulation framework that allows efficient and reliable TEG system simulations. In order to validate the model over a large range of operating conditions and not to introduce uncertainties related to heat transfer in fluids the experimental validation of the framework is done at the control surface between the CFD and TEG system in Fig. 1. This paper is organized as follows. Section 2 explains the experimental setup and Section 3 introduces the novel modeling framework. Results and discussion for modeling individual models are reported in Section 4.1 while the validation for large system of modules are found in Section 4.2. Finally conclusions are given in Section 5.

2. Measurements

An experimental setup was designed and built in order to characterize thermoelectric module performance in terms of voltage, current, and heat flow as function of temperatures and study systems of modules electrically connected together.

2.1. Experimental setup

The experimental setup consists of electrically heated aluminum blocks with one TE module on each side for symmetry reasons. The modules used are commercial bismuth telluride modules

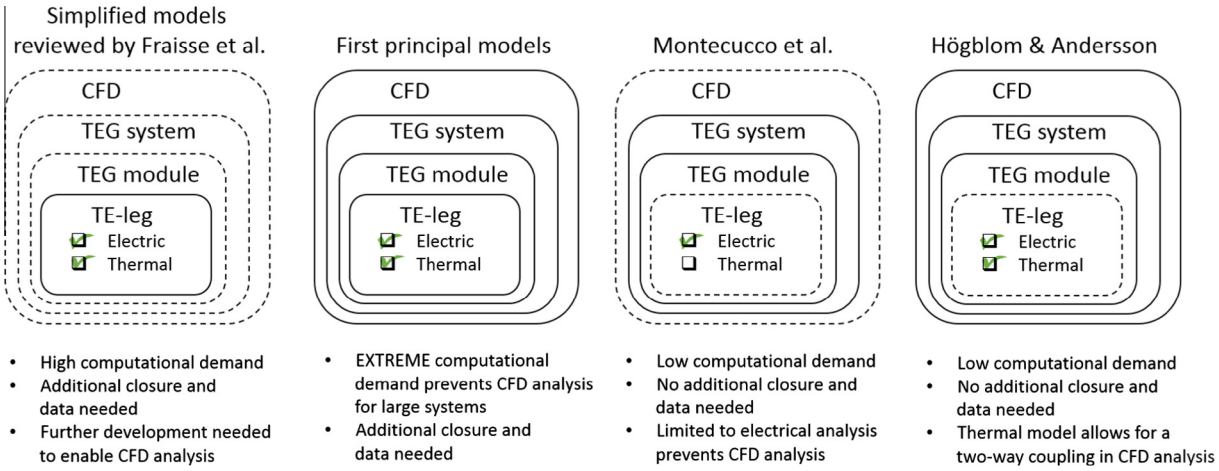

Fig. 1. Comparison between the different modeling strategies.

from Thermonamic (TEHP1-12680-0.15). The modules are 80 mm × 80 mm and consists of 126 TE pairs. On the cold side of the modules, water cooled aluminum blocks were mounted and the whole package was clamped together with springs to achieve the contact pressure specified for these modules, see Fig. 2. On either side of both modules, another aluminum block was mounted to achieve even temperatures on the module surfaces. Between all aluminum blocks and modules, high temperature thermal grease was applied in a thin layer to ensure good and even thermal contact. Two identical setups were built to be able to study modules electrically connected together but working under different thermal loads.

The electric heater was controlled using a power regulator (Kemo Power Control M028N) to support a constant power to the heater. The heat flow through the modules was achieved by measuring inlet and outlet water temperatures as well as the mass flow of cooling water through the blocks. The cooling water was fed to all the blocks in parallel from a tank at constant temperature. This tank had a slight over pressure and the mass flow of water was controlled by valves at the outlet from the cooling blocks. This caused the mass flow to be very stable with time and the uncertainty in the mass flow measurements was determined to approximately 0.2%. Temperatures measurements of the cooling water was done with thermocouples within five centimeter distance from the inlet and outlet to the blocks and the whole stack of blocks and modules were insulated to avoid thermal losses to the surrounding. In order to determine the accuracy of the temperature measurements, the inlet and outlet temperatures of the cooling water were measured at steady state when the heaters was turned off. In these measurements the difference between the inlet and the outlet temperatures was in the order of 0.05 °C. Accordingly the uncertainty in the heat flow measurements could be determined to a maximum of 1.17%, occurring at the measurement points with the lowest temperature differences. In all subsequent test when heaters were turned on the time to reach steady state was evaluated by monitoring the signal from the thermocouples.

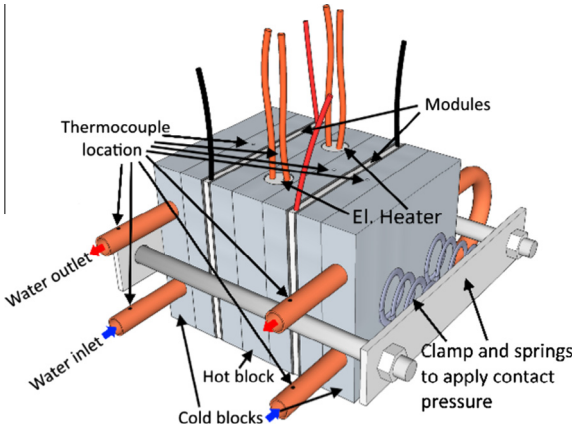

Fig. 2. Schematics of the measurement setup.

Additionally temperatures in the aluminum blocks were measured and used as boundary conditions in the simulations. The modules were connected to an electronic load, TTI LD300 (Thurlby Thandar Instruments, UK). The voltage over each module was measured as well as the current through them. The circuits were connected in series with a low resistance current shunt (1 mΩ) in order to measure current accurately without affecting the circuits more than necessary. All the data was sampled using a DataTaker DT85 (Thermo Fisher Scientific, Australia).

2.2. Individual measurements for module characterization

In the first set of measurements the modules were not connected to the load in order to study the pure Seebeck effect and heat conduction that was not influenced by any current through the circuit. For this set of measurements the electric power to the heater and thereby the temperatures in the hot blocks were varied in several small steps. During all the measurements the system was allowed to reach steady state before sampling the data.

In the next set of experiments, the individual models were connected to the load one by one and the load resistance was varied from infinite resistance (open circuit) to close to zero resistance (short circuit) while the electric power to the heaters were kept constant. This was done for different electrical power levels for each of the four modules. Repeated measurements were performed in some points which confirmed repeatability in the experiments.

2.3. System measurements for validation

For connected modules working with different temperature differences, sometimes the ones with high temperature difference forces current to flow backwards in the ones with low temperature difference. This implies that the low performing modules works as loads (Peltier coolers) to the high performing modules. When the current flows backwards in the modules they work outside the

measured range and extrapolation of the model is necessary. If the parameters are correlated, an extrapolation can lead to errors in the predicted performance. To confirm validity of the simulation method the modules were connected two and two in series and these groups were connected together in parallel to study non-ideal phenomena arising when electrically connecting modules at different temperatures work together. The power to the electrical heaters and thereby the hot side temperatures were set to be different in the two blocks to study the system when working under non-ideal thermal conditions. The results from these measurements were used to validate the models developed for the individual modules both within and also extrapolated outside their measured operating range.

Measurement of the connected system was performed at three different combinations of power levels. For each level the load resistance was varied from open to closed circuit and data sampled at steady state conditions for between 50 and 60 points at each power level. First both heaters were providing approximately the same power (700–750 W per heating element), hereinafter referred to as Case 1, thereby the temperatures of the four modules were similar. In the second series of measurements (Case 2), one of the heaters were providing less power (300–350 W per heating element) with the consequence that two of the serial connected modules were operating at lower temperature difference. Lastly in Case 3 the power of the heaters were switched and further reduced (250–300 W per heating element), the previously low temperature modules were operating at high temperatures and vice versa. Case 2 and 3 are deliberately made different to generate data for validation at different conditions. In none of the experiments the temperatures were kept constant by temperature controllers. This provides an opportunity to direct study the effect a varying current has on the temperatures, i.e. magnitude of Peltier, Thomson and Joule effects.

3. Simulation methodology

In order to develop a generic simulation framework that allows thermoelectric performance to be predicted efficiently even for a large system of modules integrated in a heat exchanger three different models are required i.e. electrical and thermal models for the individual modules and also a model for the connected system. For predicting the electrical characteristics of individual modules we introduce in accordance to the work by Montecucco et al. [34], a reduced model with some modifications to extend the range of validity by imposing a more physical model. Secondly a new model for the heat flow is developed using a similar methodology allowing the heat flow to be determined as function of temperatures and current. Finally a model for the connected system is introduced to provide a closed set of equations that can be solved implicitly.

3.1. Individual TEG characterization

For both the electrical and thermal module characterization, two different data sets were used (open circuit where temperature was varied, and closed circuit at a few temperatures where the load resistance was varied). The series of measurements on open circuit ensure there is no current flowing through the modules and thereby the measured voltage is the pure Seebeck voltage and the measured heat flow is the pure heat conduction. By using two different sets of data (open circuit and closed circuit) and by performing the regression analysis separately on these sets it is ensured that the correlation between the parameters are minimized.

In this study one set of parameters is calculated for each module, this allows small variations between modules to be accounted for. More advantageous this approach would also allow individual parameters to be determined and used if the system contains different kinds of modules.

3.1.1. Voltage model

The TE modules can be modeled as a voltage source (the Seebeck voltage) in series with an internal resistance [35,36], as shown in Fig. 3.

The total voltage over a module is thereby the Seebeck voltage minus a voltage drop depending on the internal resistance and the current flowing through the module. In work by Woo et al. [35,36] the Seebeck voltage and internal resistance was described by a linear function of the temperature difference. This was later refined in the work by Montecucco et al. [34]. In their model the Seebeck voltage and the internal resistance are described by a second order polynomial function with respect to the temperature difference with the purpose of accounting for temperature dependent material data. This is a good approach but it can be improved further by taking more physics into account. While developing a parameter model it is advantageous to include as much of the underlying physics as possible.

The Seebeck voltage is a function of the temperature difference but it is also important to account for the absolute temperature since Seebeck coefficient varies with absolute temperature. There will be temperature gradients inside the material that cannot be resolved fully with a simplified modeling approach. However the effect of absolute temperature can be included in the model by estimating the temperature inside the material from the temperatures on the cold and hot sides of the module. Knowing the hot and cold side temperatures allows the average to be determined, $T_{avg} = (T_h + T_c)/2$, where T_h and T_c are the temperatures in the hot and the cold blocks respectively. By using the block temperatures in the model, the thermal conductivity of the blocks and also the contact resistances are included in the regression model. The internal resistance is the sum of the TE material bulk resistance (depending on geometry and resistivity) and also the contact resistances. Because the resistivity in the material is temperature dependent, the total internal resistance is a function of solely the absolute temperature. The voltage over a TE module can thereby be described by:

$$U = U_{Seebeck}(\Delta T, T_{avg}) - I \cdot R_{int}(T_{avg}) \quad (1)$$

In the experimental setup used by Montecucco et al., the temperature difference were set constant by use of temperature controllers. The parameters were then determined by a linear regression analysis using the measured data of temperature

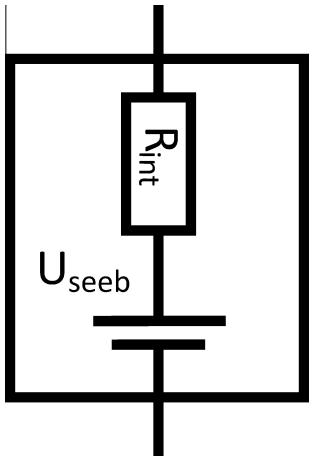

Fig. 3. Schematic model of a TE module.

difference, voltage and current through the modules, without accounting for at the absolute temperature of the modules. However it is important for a model that should be valid in a large temperature range to account for this effect since the material data, i.e. the Seebeck coefficient and electric resistivity, are dependent of the absolute temperature, not the temperature difference.

Another aspect of formulating models is that the Seebeck voltage must approach zero when extrapolating the model to zero temperature difference. In the work by Woo et al. and Montecucco et al., a constant term was included in the model for the Seebeck voltage, which effectively hinders this unless the constant term in the regression analysis equals zero. As a result the Seebeck voltage remains nonzero when extrapolating their model to zero temperature difference. Therefor we suggest an improvement to these models by removing the constant term in order to achieve a more physically model that allows for extrapolation. For this purpose and at the same time also account for the temperature dependency of the material the following model is suggested

$$U_{Seebeck} = (\beta_{s1} + \beta_{s2} T_{avg})\Delta T \tag{2}$$

where the parameters (β_{si}) are determined from the open circuit data. The dimension of the regression coefficients, β_i, obviously depend on the polynomial.

Estimations of the internal resistance then follows from subtracting the Seebeck voltage predicted by Eq. (2) from the voltage measured for a closed circuit according to Eq. (3). The internal resistance consists of two parts, the contact resistances and the materials resistivity. In order to account for the nonlinear temperature dependency the parameter model used in this study is therefore given by

$$\frac{U - U_{Seebeck}}{I} = -\left(\beta_{R1} + \beta_{R2} T_{avg} + \beta_{R3} T_{avg}^2\right) \tag{3}$$

The resulting model for the voltage can be summarized as

$$U = (\beta_{s1} + \beta_{s2} T_{avg})\Delta T - I\left(\beta_{R1} + \beta_{R2} T_{avg} + \beta_{R3} T_{avg}^2\right) \tag{4}$$

3.1.2. Heat flow model

In a similar manner, a model for the heat flow was built. The total heat flow on the cold side can be described by the sum of pure heat conduction together with the Peltier- and Thomson effect and the Joule heating that occurs when there is a current flowing through the modules.

$$Q_c = Q_{conduction} + Q_{Peltier+Thomson,cold} + Q_{Joule} \tag{5}$$

The Peltier and Thomson effect is linearly dependent on the current and the joule heating has a quadratic current dependency while the conductive part is independent of the current. By assuming the Joule heating is evenly distributed in the module, half the Joule heating will leave the module on each side. The total model for the heat flow on the cold side can therefore be written as

$$Q_c = Q_{conduction} + I\Psi_{Peltier+Thomson,cold} + \frac{I^2 R_{int}}{2} \tag{6}$$

where $\Psi_{Peltier+Thomson}$ contains a combination of the Peltier coefficient ($\Pi_{peltier}$) and the Thomson coefficient ($\tau_{thomson}$) and R_{int} is the module resistance as described earlier. The contribution from Joule heating can directly be determined by use of Eq. (3) and the measured current, i.e. $Q_{Joule} = \frac{I^2(\beta_{R1} + \beta_{R2} T_{avg} + \beta_{R3} T_{avg}^2)}{2}$. With the same approach as for determining the Seebeck voltage the heat conduction can easily be determined from measurement on open circuit. In order to ensure vanishing conductive heat flow at zero temperature difference, and at the same time allowing temperature dependent conductivity to be accounted for the following model is proposed

$$Q_{conduction} = (\beta_{F1} + \beta_{F2} T_{avg})\Delta T \tag{7}$$

Finally the measurements of the heat flow can be used to model the Peltier and Thomson effect by subtracting the conduction and Joule heating from the measured heat flow on a closed circuit.

$$Q_c - Q_{conduction} - Q_{Joule} = I\Psi_{Peltier+Thomson,cold} \tag{8}$$

For thermoelectric material, the Thomson coefficient, τ, can be expressed by the Kelvin relation as the derivative of the Seebeck coefficient with respect to temperature times the absolute temperature, $\tau = \partial\alpha/\partial T \cdot T$. Furthermore the Thomson effect is the Thomson coefficient times the current density and the temperature gradient, $q_{thomson} = \tau J \nabla T$. When combining these equations a quadratic dependency on the temperatures is apparent ($T_{avg}\Delta T$). Additionally the Kelvin relation describing the Peltier coefficient is the Seebeck coefficient times the absolute temperature, $\Pi_{peltier} = \alpha T$ which allows a model for the combined Peltier and Thomson effect to be written

$$I\Psi_{Peltier+Thomson,cold} = I(\beta_{PT1} T_c + \beta_{PT2} T_{avg}\Delta T) \tag{9}$$

The resulting models for the heat flow is given by

$$Q_c = (\beta_{F1} + \beta_{F2} T_{avg})\Delta T + I(\beta_{PT1} T_c + \beta_{PT2} T_{avg}\Delta T) + \frac{I^2\left(\beta_{R1} + \beta_{R2} T_{avg} + \beta_{R3} T_{avg}^2\right)}{2} \tag{10}$$

Eq. (10) describes the heat flow on the cold side of the module. At steady state, the heat flow entering the module on the hot side is the same but with one additional term describing the heat flow converted to electric energy, $P_{el} = IU = I(\beta_{s1} + \beta_{s2} T_{avg})\Delta T - I^2(\beta_{R1} + \beta_{R2} T_{avg} + \beta_{R3} T_{avg}^2)$. When this is inserted in Eq. (10), the heat flow on the hot side can be expressed as

$$Q_h = (\beta_{F1} + \beta_{F2} T_{avg})\Delta T + I(\beta_{PT1} T_c + \beta_{PT2} T_{avg}\Delta T) + I(\beta_{s1} + \beta_{s2} T_{avg})\Delta T - \frac{I^2\left(\beta_{R1} + \beta_{R2} T_{avg} + \beta_{R3} T_{avg}^2\right)}{2} \tag{11}$$

It should be noted that the Peltier Thomson term on the hot side is the sum of the second and the third term in Eq. (11), i.e. $Q_{Peltier+Thomson,hot} = Q_{Peltier+Thomson,cold} + IU_{Seebeck}$.

Thereby the difference between the heat flow into the module on the hot side and out from the module on the cold side exactly corresponds to the net electric power generated by the thermoelectric modules when the Peltier effect and the Joule losses are taken into account. The formulation of the model allows steady state analysis, however allowing for transient analysis would also require an accumulation term to account for the thermal mass of the modules.

Both the Seebeck coefficient, the resistivity and the thermal conductivity all have a nonlinear temperature dependency. Different order polynomial were considered and the correlation between the parameters were evaluated. The choice of the models suggested above is based on a low degree of correlation. If higher order polynomials were chosen, the higher correlation between the parameters would result in a model with higher predictability in the measured operating range but it would potentially be less accurate when extrapolated outside the operating range where the model is developed. For the internal resistance, a low correlation allowed for a 2nd order polynomial to be used but in the other models lower order terms were chosen to keep the correlations low and allow for extrapolation.

3.2. Model of system with connected modules

A model for the connected system is introduced to provide a closed set of equations that can be solved implicitly. A diagram of a general system of m serial connected groups, each containing n modules, is shown in Fig. 4.

For a given load resistance, surface temperatures and the relationship between voltage and current for single modules described by Eq. (4), it is straightforward to derive a model for any system of connected modules. U_{tot} is given by the sum of voltages in any of the serial connected groups

$$U_{tot} = \sum_{j=1}^{n} U_{ji} \quad \forall i \in \{1, \ldots, m\} \tag{12}$$

where the voltage over each module, U_{ji}, is the Seebeck voltage minus the Ohmic voltage drop according to Eq. (4), which for the generic system is formulated as

$$U_{ji} = U_{seebeck,ji} - I_i R_{ji} \quad \forall i \in \{1, \ldots, m\}, j \in \{1, \ldots, n\} \tag{13}$$

Furthermore, by using Ohm's law, the load current is given by

$$I_{load} = U_{tot}/R_{load} \tag{14}$$

which equal the sum of current in the different groups according to Kirchhoff's current law

$$I_{load} = \sum_{i=1}^{m} I_i \tag{15}$$

Given a temperature difference, $U_{seebeck,j,i}$ and R_{ji} can be calculated for each module since they are independent of the current. Thereafter, the equation system, Eqs. (12)–(15) containing a total of $(n+1)m+2$ unknown (U_{tot}, U_{ji}, I_{load} and I_i) and the same number of equations, can be solved. This is under assumption that the load resistance, R_{load} is known. In order to maximize the electrical power output, the load resistance should match the resistance in the connected system of modules, i.e. it can be calculated as

$$R_{load} = \frac{1}{\sum_{i=1}^{m}\left(\frac{1}{\sum_{j=1}^{n} R_{ji}}\right)} \tag{16}$$

Since none of the currents in the groups $(I_1, \ldots, I_m)$ are known, (in general) these equations has to be solved in an iterative manner. Knowledge of the current through the different groups allows the heat flows to be determined by Eqs. (10) and (11).

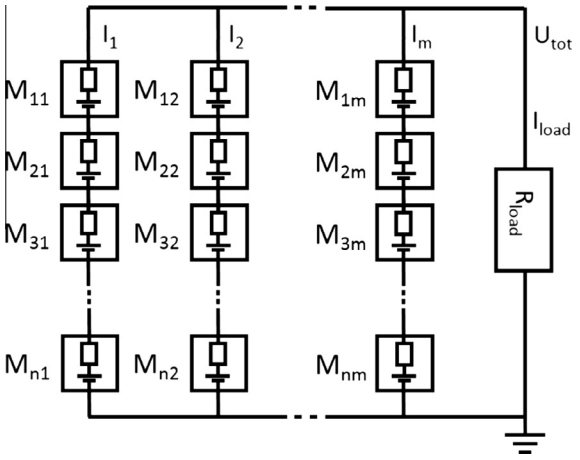

Fig. 4. Schematics of general system of $n \cdot m$ modules.

3.3. CFD implementation

When using these models in a CFD environment, the temperatures are not known in advance rather solved for in an iterative manner together with the other flow variables. This means a two-way coupling in the energy equation is made possible by applying these models and using heat flow boundary conditions on the TEG surfaces in the CFD model.

In a CFD analysis, a one way coupling in the energy equation would mean that TE modules are simulated with an efficient heat conductivity to achieve the temperature distribution. Thereafter, the thermoelectric generation would be solved for as a post processing operation. This approach effectively hinders the Peltier, Thomson and Joule effects to be accounted for correctly since the generated current can never affect the temperature field. On the contrary, by using a two-way coupling in the energy equation, meaning the flow and temperature fields are solved simultaneously with the thermoelectric generation, the heat flow caused by the Peltier, Thomson and Joule effects can be accounted for correctly.

A block diagram describing the calculation procedure, allowing two-way coupling of the energy flow is shown in Fig. 5.

As shown in Fig. 5 the TEG model requires input regarding the electrical connections and the load resistance. The generic formulation of the model allows flexible implementation of different type and number of modules, and also any electrical configuration. Furthermore, it requires the module parameters $(\beta_{s1}, \beta_{s2}, \beta_{R1}, \beta_{R2}, \beta_{R3}, \beta_{F1}, \beta_{F2}, \beta_{PT1}, \beta_{PT2})$ described in Section 3.1. Once every iteration the temperatures in the cold and hot blocks adjacent to all modules are read by the subgrid TEG model and the temperature difference and average temperature are determined for each module in the system, thereby allowing Seebeck voltages and internal resistances to be calculated using Eqs. (2) and (3). Information about these along with external load resistance, and specification on electrical connections allows the current distribution in the system to be calculated using Eqs. (12)–(15). Having the current through all the modules determined, the heat flow on either sides of the modules can be calculated with Eqs. (10) and (11). The heat flow on the modules hot and cold sides are sent back to the CFD solver where they are implemented as heat flux boundary conditions that is directly linked with the module surfaces in the CFD model i.e. $Q_{c,ji}$ $Q_{h,ji}$.

4. Results and discussion

Fig. 6a shows the measured electric power-current characteristics for one of the modules colored by the temperature difference that is used in the regression analysis to determine the model parameters. The black curves shows the simulated power for the same conditions. As shown here the model fits the measurements very well in the whole measured temperature range. Fig. 6b shows the modeled heat flow versus the measured heat flow for the same module. Although the heat flow is more challenging to measure correctly compared to the electric characteristics the agreement is very good, and the model has no apparent lack of fit.

Tests were done to confirm no hysteresis exist, by measuring over the entire measurement range and then back to confirm same results were obtain when starting all over.

4.1. Validation of individual modules

The models for the individual thermoelectric modules fits the experimental data very well. The coefficient of determination, R^2, is a statistical measure of how well a model fit experimental data and it is defined as the ratio of the variance explained by the model

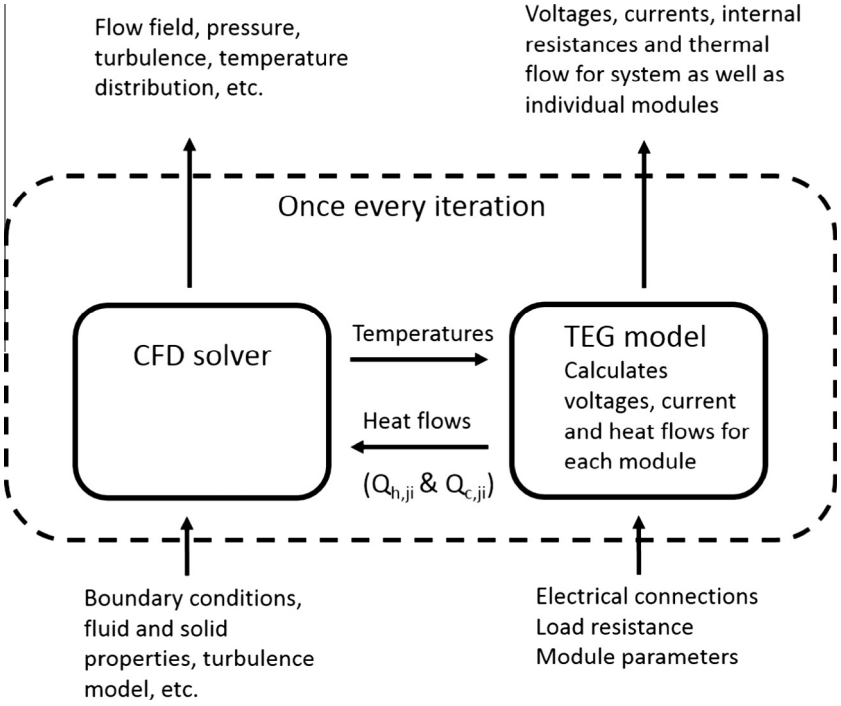

Fig. 5. Schematic of calculation procedure.

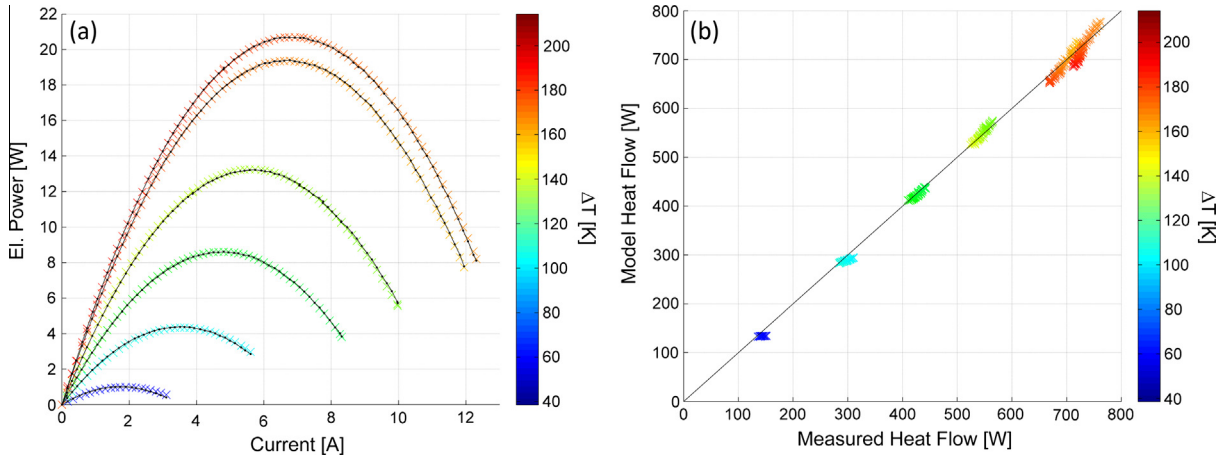

Fig. 6. (a) Measurements (colored by ΔT) and simulations (black) of electric power from a module versus current. (b) Modeled heat flow versus measured heat flow colored by ΔT.

to the total variance in the measurements. Adjusted R^2 is a modification of R^2 where the number of explanatory variables are taken into account. Comparison between the R^2 and adjusted R^2 is thereby a measure of whether the model is over parametrized [37]. The following statistical analysis is done in Matlab. R^2 for voltage and heat flow for the suggested model is summarized in Table 1 together with the corresponding adjusted R^2, which all confirm very good agreement between measurements and models.

As shown in Table 1 the high R^2 values ($\geqslant$99.4%) shows that the model allows very accurate prediction of thermal and electrical performance. A statistical variance analysis based on the repeated experiments shows that contributions to the variance from repeated experiments is actually so low it gives a high test value for model lack of fit, significant on 99% level. As a consequence of very repeatable experiments i.e. very low noise, the statistical analysis actually show the model could be improved. Furthermore the

Table 1
Coefficient of determination.

	Module 1		Module 2		Module 3		Module 4	
	Voltage	Heat flow	Voltage	Heat flow	Voltage	Heat flow	Voltage	Heat flow
R^2	0.99947	0.99556	0.99903	0.99803	0.99913	0.99648	0.99979	0.99793
R^2adj	0.99947	0.99551	0.99902	0.99801	0.99912	0.99644	0.99979	0.99791

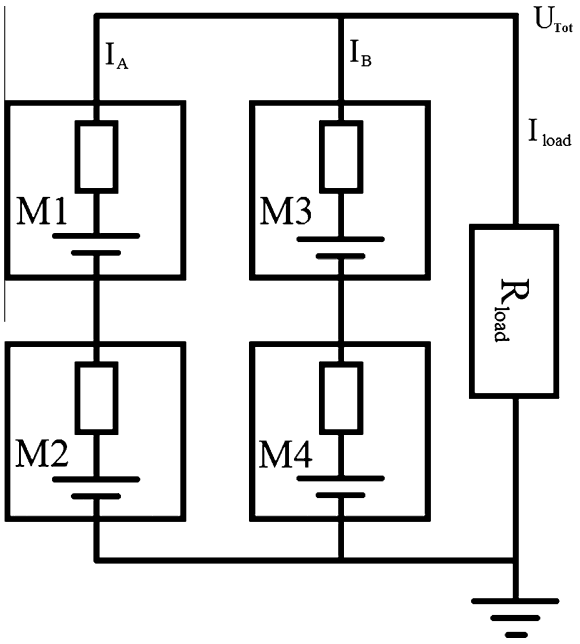

Fig. 7. Schematics of the connected system used for validation.

adjusted R^2 values are very similar to the R^2 which show the model is far from over parametrized, and the model could potentially include more terms. It is however difficult to find physical motivation introducing additional terms in the model. More terms could potentially improve the R^2 values further. However, at the same time it could lead to less accurate prediction when used to extrapolate outside the region where the model was originally developed. This risk and also the low potential in improving the model further (maximum improvement is 0.6% since the model already explains 99.4% of all variance) leads to the conclusion the model is physically motivated and gives sufficient accuracy.

4.2. Validation of the simulation framework

The system of connected modules described in Section 2.3 was simulated and compared with measurements at the same thermal conditions. Validation of the simulation method was done over a large range of operating conditions, even when some modules in the system counter act thermoelectric production and work as Peltier coolers. The experiments were therefor done with significantly different thermal conditions to really stress the model and allow assessment of how good it works when extrapolating into these non-ideal operating conditions. A schematic diagram describing the connected system is shown in Fig. 7.

For the system shown in Fig. 7, evaluation of the thermal and electrical performance requires a solution of the implicit equation system, Eqs. (12)–(15) to determine the currents. In this system we have 2 serial connected groups, each containing 2 modules, consequently a total of $(n+1)m+2=8$ unknowns (U_{tot}, U_1, U_2, U_3, U_4, I_{load} and I_A, I_B) and the same number of equations since Eq. (12) provides 2 relationships, Eq. (13) provides 4 relationships, and Eqs. (14) and (15) provides 1 relationship each. Solution of this

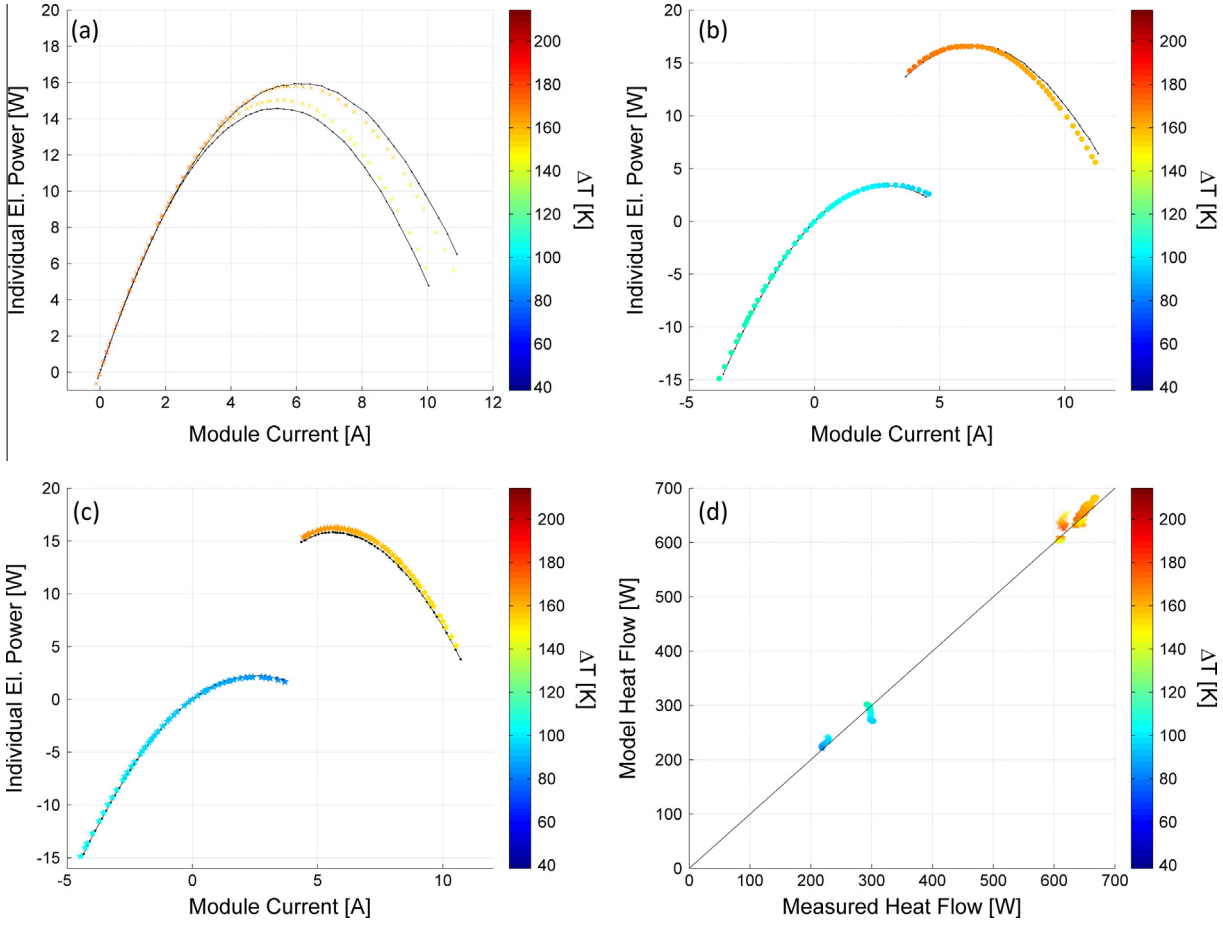

Fig. 8. Measurements (colored by ΔT) and simulations (black) of electric power from individual modules versus module current, I_A, and I_B. (a) Case 1, (b) Case 2, (c) Case 3, (d) Modeled heat flow versus measured heat flow colored by ΔT. (For interpretation of the references to colour in this figure legend, the reader is referred to the web version of this article.)

equation system requires information about the Seebeck potentials and internal resistances, i.e. 2 characteristics of each modules that are explicitly determined by Eqs. (2) and (3) given the measured temperatures. The voltage over each module, and the currents through each group can therefor directly be used for validation of the models. Information about the currents subsequently allow the heat flow on the cold sides to be calculated from Eq. (10) for each module, and used for validation as well. Hence in total 20 unknowns and 20 relationships is solved iteratively for validation of this relatively small system. Even for larger systems of modules, with significantly more unknowns, the solution of the resulting implicit equation system is easy. This means that the additional cost of implementing this modeling framework in a CFD analysis results in a minor increase in computational demand.

In Fig. 8a–c the electrical power contribution from the different modules is depicted as function of the current through them for the three different combinations of power levels described in Section 2.3. The same color scale is used to visualize the temperature difference the modules are operating at.

The differences between the hot and cold surfaces of the modules are clearly visible by color scale in Fig. 8. However, the relatively small change of temperature that occurs as a result of the varying current is difficult to read out from this color scale. In Case 1 temperature differs approximately 30 K between open and closed circuit. While in Case 2 and 3 temperature variations are lower, typically 15–20°. This can be explained by non-vanishing Peltier effect for these cases as there will be current through the modules even for an open circuit, as a consequence of the electrical connection. When the modules are operating at different temperatures, it is obvious that the modules sometimes have a negative contribution to the systems total electrical power output i.e. Fig. 8b–c.

Fig. 8d shows the corresponding modeled heat flow versus the measured heat flow. There are slightly larger deviations for the heat flow compared to the electrical characteristics. But overall the accuracy is satisfying and there is no clear correlation between temperature difference and the deviations. The larger deviations might be explained by the fact it is more difficult to measure heat flow compared to the voltage and current, as already indicated in Table 1.

In Fig. 9a–c the electrical power output from the different modules are shown as function of the total current through the load. Fig. 9d shows comparison between the predicted power generation and the measured power generation for the entire systems as function of the current through the load for the three different cases.

For open circuits, when there is no load current, the total power output is naturally zero but as seen in Fig. 9b and c, the individual contributions are positive (≈15 W) for the modules with high temperature difference, and negative (≈−15 W) for the modules with low temperature difference. This implies the low performing modules operates as Peltier coolers and the current generated by the high performing modules pumps heat from the cold to the hot side in the low performing modules. When closing the circuit and thereby allowing a current through the load useful power is gener-

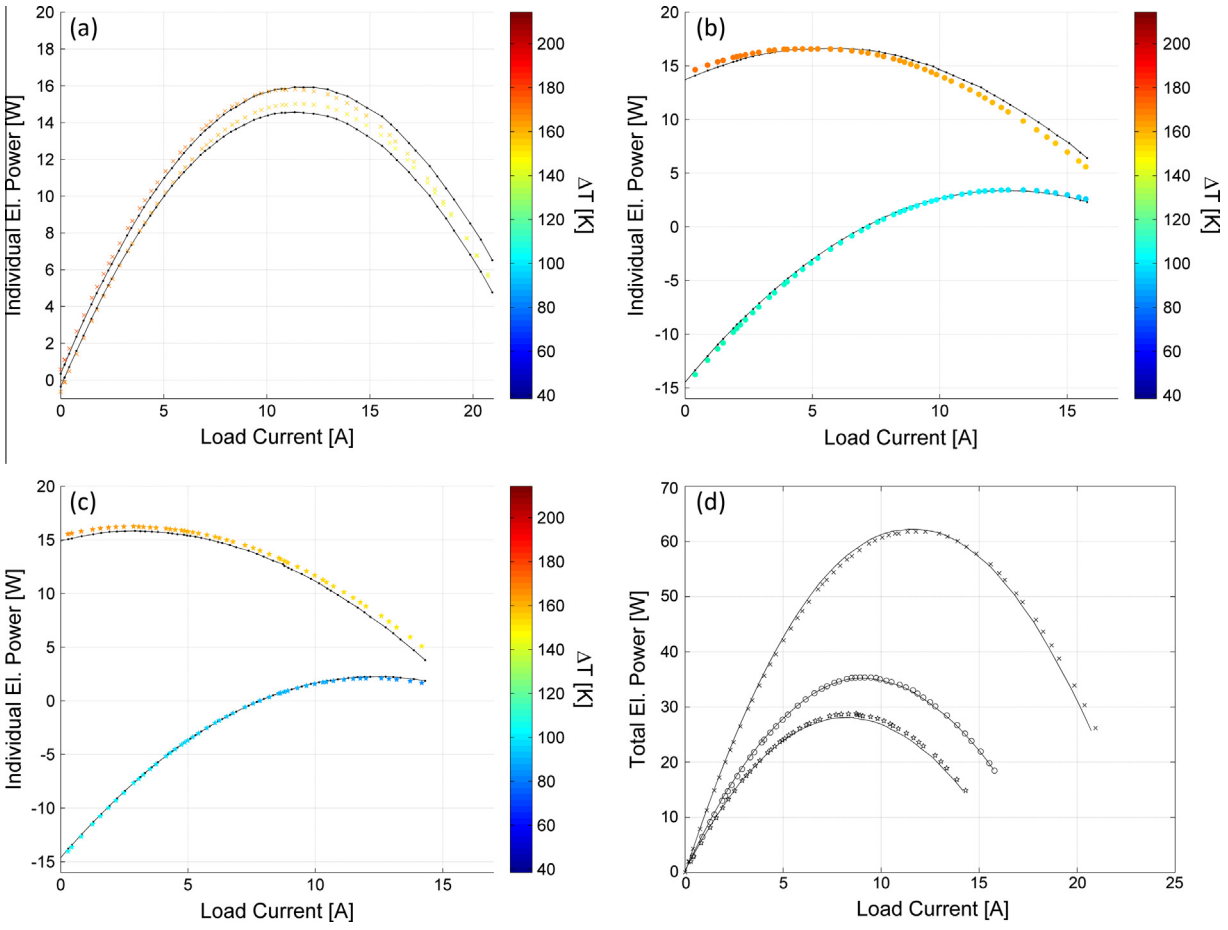

Fig. 9. Measurements (colored by ΔT) and simulations (black) of electric power from individual modules versus load current. (a) Case 1, (b) Case 2, (c) Case 3, (d) Measurements and simulations (solid lines) of total electric power from all modules versus load current for Case 1–3. (For interpretation of the references to colour in this figure legend, the reader is referred to the web version of this article.)

Table 2
Statistical evaluation, R^2 values determined for the connected system.

	Module 1	Module 2	Module 3	Module 4
Voltage	0.995624	0.996761	0.998179	0.996940
Current	0.99959	0.99959	0.99962	0.99962
Heat flow	0.99205	0.99505	0.99287	0.97446

ated. It reaches its maximum when the load resistance equals the overall resistance in the system of connected modules in accordance with the maximum power theorem [38]. It should be noted that there is a constant power to the electric heater for each curve in Figs. 8a–c and 9a–c. When the current is flowing through the modules, the Peltier, Thomson and Joule effects gives rise to a slight change in temperatures on the module surfaces. Since steady state is reached in each point and the temperatures are measured correspondingly, this change in temperature is taken into account both when developing the model and during validation in the connected system, due to the model being formulated as dependent on both absolute and temperatures difference over the modules.

It is concluded that the simulation framework proposed here allows very good agreement between thermal and electrical performance for the wide range of operating conditions. A statistical evaluation of the entire data set, i.e. all the four modules used in the three different cases, shows that the model allows 99.6% and 99.9% of the variance in voltage and current respectively and 97.4% of all variance in the heat flow to be predicted, as summarized in Table 2.

As shown in Table 2, the R^2 values for the current is identical for module 1 and 2 as well as for module 3 and 4. This is expected since the current through them is the same (I_A and I_B).

When designing a large TEG system for heat recovery from waste streams of liquids or gases it is a very likely that the modules will operate under different thermal conditions since the energy content will be reduced substantially from the inlet to the outlet. This can partly be compensated for by increasing the heat transfer from the fluid closer to the outlet. The simulation framework proposed here can directly be used to design the electrical connections, in order to minimize the non-ideal effects arising from modules working under significant different temperature conditions. In many applications e.g. automotive heat recovery in exhaust gases, the available energy in the gases, i.e. temperatures and flowrates will also change with time [14]. It is preferable to have a stable voltage from the system suitable for the specific application which calls for methods to control the total output voltage. This can be done with various techniques such as different DC–DC converters or using high frequency switching between serial and parallel connections. By use of a flexible transistor based switching network together with the models presented in this work and inline measurements of the temperatures, a control strategy could be developed which allows for stabilizing output voltage while at the same time minimizing the non-ideal effects discussed in this work.

5. Conclusion

A simulation methodology for characterization and simulation of TEG systems allowing accurate prediction of TEG voltage and current as well as heat flow at steady state was successfully developed. Following the modeling strategy proposed in the literature a new model was proposed that allows the performance for a wider range of operating conditions to be predicted by introducing a more physical model. This included both temperature dependent material data and consistent behavior of Seebeck potential at low temperature differences.

In order to allow a multiscale simulation approach in fluid dynamics simulation a novel model for heat flow was developed and implemented in the simulation framework. This models are based on measurement and analysis of the contribution from heat conduction, Peltier, Joule and Seebeck on electrical and thermal performance of modules. It allows internal contact resistances and temperature dependent material data to be taken into account without explicit characterization. Experimental validation was done on a system with electrical connected modules working at various temperature and current ranges. It is concluded that the predictions are very good even under highly non-ideal conditions with reversed current, i.e. modules operating as Peltier coolers rather than generators. Statistical evaluation confirmed that the model allows 99.6% of the variance in voltage and 97.4% of all variance in the heat flow to be predicted, including extrapolation into regions where the original model was not developed.

The good performance was attributed to the physical formulation of model. Hence, the proposed simulation framework provides an adequate description of the physics although a significant reduction of the computational demand is achieved by scale separation, i.e. the internal parts does not need to be resolved. This provides a possibility to predict thermoelectric generation in systems where the local heat flow is modeled by use of CFD analysis, since for most engineering applications a first principle approach would be far too computational demanding.

In such cases the models presented here would be introduced as subgrid models to allow two-way coupling in the energy equation in a computational efficient way. Consequently the simulation framework is able to bridge the scale separation problem and allows heat flow and electric power generation to be determined accurately.

Acknowledgement

This work was financially supported by the Swedish Foundation for Strategic Environmental Research.

References

[1] Nuwayhid RY, Shihadeh A, Ghaddar N. Development and testing of a domestic woodstove thermoelectric generator with natural convection cooling. Energy Convers Manage 2005;46(9–10):1631–43.
[2] O'Shaughnessy SM et al. Field trial testing of an electricity-producing portable biomass cooking stove in rural Malawi. Energy Sustain Dev 2014;20:1–10.
[3] Champier D et al. Study of a TE (thermoelectric) generator incorporated in a multifunction wood stove. Energy 2011;36(3):1518–26.
[4] Py X, Azoumah Y, Olives R. Concentrated solar power: current technologies, major innovative issues and applicability to West African countries. Renew Sustain Energy Rev 2013;18:306–15.
[5] Liao TJ, Lin BH, Yang ZM. Performance characteristics of a low concentrated photovoltaic–thermoelectric hybrid power generation device. Int J Therm Sci 2014;77:158–64.
[6] Ji J et al. A sensitivity study of a hybrid photovoltaic/thermal water-heating system with natural circulation. Appl Energy 2007;84(2):222–37.
[7] Zhang M et al. Efficient, low-cost solar thermoelectric cogenerators comprising evacuated tubular solar collectors and thermoelectric modules. Appl Energy 2013;109:51–9.
[8] He W et al. Parametrical analysis of the design and performance of a solar heat pipe thermoelectric generator unit. Appl Energy 2011;88(12):5083–9.
[9] Suter C, Jovanovic ZR, Steinfeld A. A 1 kWe thermoelectric stack for geothermal power generation – modeling and geometrical optimization. Appl Energy 2012;99:379–85.
[10] Whalen SA, Dykhuizen RC. Thermoelectric energy harvesting from diurnal heat flow in the upper soil layer. Energy Convers Manage 2012;64:397–402.
[11] El-Genk MS, Saber HH. Performance analysis of cascaded thermoelectric converters for advanced radioisotope power systems. Energy Convers Manage 2005;46(7–8):1083–105.
[12] Wang Y, Dai C, Wang S. Theoretical analysis of a thermoelectric generator using exhaust gas of vehicles as heat source. Appl Energy 2013;112:1171–80.
[13] Högblom O, Andersson R. CFD modeling of thermoelectric generators in automotive EGR-coolers. Am Inst Phys Conf Ser 2011;1449:497–500.
[14] Espinosa N et al. Modeling a thermoelectric generator applied to diesel automotive heat recovery. J Electron Mater 2010;39(9):1446–55.

[15] Deng YD, Zhang Y, Su CQ. Modular analysis of automobile exhaust thermoelectric power generation system. J Electron Mater 2015;44(6):1491–7.
[16] Yu SH et al. Start-up modes of thermoelectric generator based on vehicle exhaust waste heat recovery. Appl Energy 2015;138:276–90.
[17] Kaibe H, et al. Thermoelectric generating system attached to a Carburizing Furnace at Komatsu Ltd., Awazu Plant. In: Paraskevopoulos KM, Hatzikraniotis E, editors. 9th European conference on thermoelectrics; 2012, Amer Inst Physics: Melville. p. 524–7.
[18] Siviter J et al. Megawatt scale energy recovery in the Rankine cycle. IEEE Energy Convers Congress Exposition (ECCE) 2012;2012:1374–9.
[19] Chen M, Rosendahl LA, Condra T. A three-dimensional numerical model of thermoelectric generators in fluid power systems. Int J Heat Mass Transf 2011;54(1–3):345–55.
[20] Chen WH, Liao CY, Hung CI. A numerical study on the performance of miniature thermoelectric cooler affected by Thomson effect. Appl Energy 2012;89(1):464–73.
[21] Cheng CH, Huang SY. Development of a non-uniform-current model for predicting transient thermal behavior of thermoelectric coolers. Appl Energy 2012;100:326–35.
[22] Ziolkowski P et al. Estimation of thermoelectric generator performance by finite element modeling. J Electron Mater 2010;39(9):1934–43.
[23] Hu XK et al. Three-dimensional finite-element simulation for a thermoelectric generator module. J Electron Mater 2015;44(10):3637–45.
[24] Rezania A, Rosendahl LA. A comparison of micro-structured flat-plate and cross-cut heat sinks for thermoelectric generation application. Energy Convers Manage 2015;101:730–7.
[25] Rowe DM, editor. CRC handbook of thermoelectrics. CRC Press LLC; 1995.
[26] Nolas GS, Sharpc J, Goldsmid HJ. Thermoelectrics: basic principles and new materials developments. New York; 2001.
[27] Bjørk R. The universal influence of contact resistance on the efficiency of a thermoelectric generator. J Electron Mater 2015;44(8):2869–76.
[28] Ebling D et al. Module geometry and contact resistance of thermoelectric generators analyzed by multiphysics simulation. J Electron Mater 2010;39(9):1376–80.
[29] Högblom O, Andersson R. Analysis of thermoelectric generator performance by use of simulations and experiments. J Electron Mater 2014:1–8.
[30] Wang Y et al. Optimization of fin distribution to improve the temperature uniformity of a heat exchanger in a thermoelectric generator. J Electron Mater 2015;44(6):1724–32.
[31] Martínez A et al. Optimization of the heat exchangers of a thermoelectric generation system. J Electron Mater 2010;39(9):1463–8.
[32] Fraisse G et al. Comparison of different modeling approaches for thermoelectric elements. Energy Convers Manage 2013;65:351–6.
[33] Montecucco A, Knox AR. Accurate simulation of thermoelectric power generating systems. Appl Energy 2014;118:166–72.
[34] Montecucco A, Siviter J, Knox AR. The effect of temperature mismatch on thermoelectric generators electrically connected in series and parallel. Appl Energy 2014;123:47–54.
[35] Rowe DM, Min G. Evaluation of thermoelectric modules for power generation. J Power Sources 1998;73(2):193–8.
[36] Woo BC et al. Characteristic of maximum power with temperature difference for thermoelectric generator. In: Proceedings of twentieth international conference on thermoelectrics, IEEE, New York. p. 431–4.
[37] Rasmuson A et al. Mathematical modeling in chemical engineering. Cambridge: Cambridge University Press; 2014.
[38] Montecucco A et al. Simple, fast and accurate maximum power point tracking converter for thermoelectric generators. IEEE Energy Convers Congress Exposition (ECCE) 2012;2012:2777–83.